Investigation and Modeling of Equilibrium Plasma for Spherical Flame Initiation and Measurements

James Shaffer¹ and Omid Askari.²
West Virginia University, Morgantown, WV, 256505, USA

Laminar flame speeds at high pressure are difficult to experimentally observe. Typically, high-pressure flame diagnostic is accomplished through observation of a spherically expanding flame in a constant volume chamber. However, flame instabilities at large radius and ignition effects at small radius limit measurable pressure range for Laminar flame speeds. Advanced combustion devices which operate at high pressures to improve capabilities and efficiencies require high quality laminar flame speed to aid in simulations and development. To expand the measurable range of flame data for high pressure flame measurement, this study proposes the further investigation of the ignition source and the incorporation of ignition diagnostics into the traditional flame speed analysis. To achieve this goal in future research, experimental spark propagation is observed and described in detail with the goal of improved experimental control and understanding. Parameters such as pressure, composition, electrode geometry and surface quality are discussed and the implication it has on the observed schlieren kernel propagation. Careful preparation of the ignition source can lead to improved surface and shape for future flame measurements. It is also shown that the thermal energy dissipated into the gas during discharge can be captured experimentally through measurement of the spark voltage, current and plasma sheath voltage drop. With the experimentally captured thermal energy, a simple energy balance can be used to describe the size of the observed ignition kernel for radius larger than 0.3 mm (following breakdown). The measurement of the thermal energy is described utilizing two experimental methods to find the discharge voltage of the nonequilibrium region at the boundary of the electrodes.

I. Introduction

Thermal spark plasma is studied at high pressure. While the details specified here are specifically relevant to fundamental combustion science, further understanding of thermal plasma propagation is relevant to many fields and industries, including combustion [1], chemical conversion [2], flame stabilization [3], health care [4], manufacturing and surface treatment [5] to name a few. This work presented aims to further understand and characterize how spark discharge plasma manifests as relevant to spherically propagating flames. has the goal of providing preliminary work necessary to address high pressure flame speed measurement (where flame instabilities are of concern) by observing the early kernel propagation (0.2-6mm) which is known to remain laminar even at high pressures [3]. Typically, the data during the early flame stage discarded to avoid ignition influence. It is proposed in a separate work that the total experimentally observed flame velocity is the sum of the flame and ignition propagation such that if ignition without flame can be accurately predicted and quantified, the available flame propagation models can be updated to include the addition of plasma affects. Since ignition can occur without flame this work will solely explore the spark discharge to develop the information necessary to capture quantitative information for future early flame measurements. It is proposed that a simple thermodynamic model can describe the size and growth of the ignition kernel using experimentally measured spark power.

¹ PhD Candidate, Mechanical and Aerospace Engineering Department.

² Associate Professor, Mechanical and Aerospace Engineering Department.

II. Model Description

The thermodynamic model solves the energy and mass conservation equations to find the radius, mass, and averaged temperature of the ignition kernel. A schematic of the model is shown in Figure 6 where the dashed control volume is defined as the ignition kernel edge with energy entering and exiting the system uniformly over the entire volume.

Assumptions for the thermodynamic model include: (a) unburned and burned gases behave as an ideal gas; (b) it is assumed that the kernel is approximately spherical; (c) since the relaxation time scale of different energy modes compared to plasma expansion time is small (~ 10-9 s), all species are in local thermodynamic equilibrium [6–10]; (d) the modeling begins shortly after the breakdown; (e) the only mass gain occurs from thermal diffusion of the ignition kernel; (f) the radial temperature profile can be assumed linear; and (g) spark energy losses result from thermal radiation, heat conduction and sheath formation.

The model begins with energy balance,

$$m_b \frac{dh_b}{dt} + \frac{dm_b}{dt} h_b = \dot{E}_{net} + \dot{m}_i h_u \tag{1}$$

where m is the mass, h is the enthalpy, \dot{m} is the mass flow rate, subscript b represents the gas heated by the plasma channel, subscript u refers to the surrounding gas, and i is the entering conditions. \dot{E}_{net} is the thermal power discharged by the spark where effects of radiation, electrode conduction and plasma losses are removed. Plasma losses are considered to occur in the plasma sheath where the loss in the sheath can be characterized by the voltage drop across this region.

By solving the energy balance for the change in kernel temperature under constant pressure conditions, we find,

$$\frac{dT_b}{dt} = \frac{\dot{E}_{net} + \dot{m}_b(h_u - h_b)}{m_b c_{pb}} \tag{2}$$

where $\dot{m}_b = \dot{m}_i$ (the mass entering the ignition kernel) is a result of thermal diffusion, T is the temperature and c_p is the mixture specific heat at constant pressure. This is the form of the first governing equation that can be integrated to find the average temperature of the kernel over time using the deposited thermal energy. The ideal gas equation can be used to solve for the kernel volume. All thermodynamic properties are calculated for a wide range of temperatures from Askari et al. [11,12]. It should be noted that the ideal gas equation can be differentiated and combined with Eq.(2) to directly solve for the kernel velocity shown in Eq. (3), where A is the kernel area and Ω is a tabulated thermodynamic property from [11,12]. However, it is more beneficial to solve directly for the temperature.

$$\frac{dr_b}{dt} = \left(\frac{1}{c_p T_b} + \frac{\Omega}{R c_p}\right) * \frac{\dot{E}_{net}}{\rho A} + \left[\left(\frac{1}{c_p T_b} + \frac{\Omega}{R c_p}\right) (h_u - h_b) + 1\right] * \frac{\dot{m}_b}{\rho A}$$
(3)

Thermal diffusion through the gas is assumed the primary mechanism for kernel expansion. Therefore, from the energy balance perspective, the energy associated with the mass gain by the kernel propagation $\dot{Q} = \dot{m}_b(h_b - h_u)$ should be equal to the energy flux by thermal diffusion through the Fourier heat equation which results in,

$$\dot{m}_b = \frac{Ak \frac{T_b - T_u}{1/4r}}{h_b - h_u} \tag{4}$$

III. Methods

Experiments are conducted using a constant volume combustion chamber (CVCC). The CVCC has an internal volume with a diameter and height of 13.3 cm and uses polished quartz disks on either end to provide optical access to the ignition kernel. The experimental diagnostic includes a linear Toepler-type Schlieren system The light source is a red 625 nm Thorlabs led (model M625L4), which is collected with an initial lens (Lens 1) and focused through a 1 mm diameter pinhole to remove excess stray light and make the light as close to a uniform point source as possible. After the pinhole, a plano-convex lens (Lens 2), with a 20 cm focal length, is used to pass collimated light through the plasma discharge, and another plano-convex lens (Lens 3), having a 40 cm focal length, for converging the light over the camera sensor. The Photron FASTCAM SA-Z high-speed camera is utilized to take images during the plasma formation (15,000 fps at 640×640-pixel resolution).

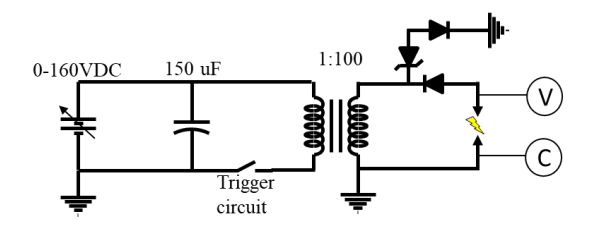


Fig. 1 Simplified circuit diagram for spark generation

The ignition system utilizes a 150 *uF* capacitor and a 100:1 automotive ignition coil to provide variable spark energies to the experiment. The spark electrical characteristics are measured using a NorthStar PVM-4 high-voltage probe and a Pearson 6595 current ring. Glow and arc discharges with varying intensities are possible over the observed pressure range. The electrodes are 0.5 mm stainless steel wire which have been polished using 5000 - 46000 Grit polishing media. For Kernel modeling results the gap is selected to be small, at around 0.2 mm to minimize the effect of breakdown. For plasma measurements various gap sizes and in general use a zero-length [13] extrapolation to estimate the properties reported. All results are captured at room temperature of 300K.

IV. Results

The results are separated into 3 sections, A brief discussion of the kernel morphology, The measurement of plasma characteristics, and modeling results of a few selected spark conditions shown in Table 1. The plasma characteristics are captured for glow discharge up to 3 atm observe the effects of the electrode surface quality and gas composition. Are discharge is observed over a wide range of parameters up to 20 atm but did not vary significantly with most conditions

Case Number #	Composition	Pressure (atm)	Voltage Drop in Glow (V)	Voltage Drop in Arc (V)	Percent Arc
1	Air	1	330	N/A	0%
2	$N_2 + CH_4$	1	348	15	10%
3	Air	3	320	N/A	0%
4	Air	5	305	40	53%

Table 1. Observed experimental conditions for modeling results

A. Kernel Morphology

Many parameters effect overall kernel morphology, electrode geometry, surface quality (i.e., roughness), gas pressure, ignition circuit (i.e., current discharge profile), and gap size. Fig. 2 illustrates some of the most significant effects along-side a sample of the spark waveform. A significantly energetic breakdown phase of the spark will result in the toroidal shape seen on the left in Fig. 2 (a result of large discharge gap). Modeling does not account for breakdown so this is minimized experimentally. Arc and glow discharge have the potential to exist for any duration of time up to 0.7 ms.

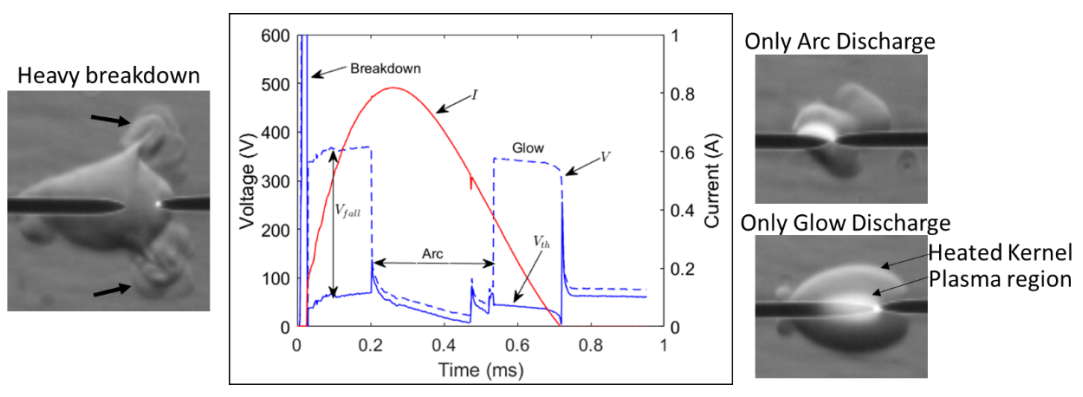


Fig. 2 Discharge voltage and current characteristic waveforms with effect on kernel morphology.

The plasma formed by arc discharge (Fig. 2, top right) is often not symmetric about the electrode which results in irregular kernels making size measurements challenging. The transition to arc discharge occurs from increased surface temperatures at the electrode which can be prevented through polishing the electrode with high grit papers and paste (all glow discharge was lost after ~5atm). A kernel which operates in glow discharge with no transitions to arc plasma are observed to maintain a smooth and uniform kernel. It is important to maintain the volumetric discharge of glow plasma (where possible) for this work to achieve high quality kernel size measurements.

B. Plasma Loss Measurements

Zero length extrapolations were used to measure the voltage drop across plasma sheath formations at the conditions relevant to the modeling results. In Fig. 3 the effects of composition and surface quality are shown. The quality of the electrode was noted to change through two mechanisms, preparation methods prior to measurement, and effects of the plasma on the surface after significant number of discharges.

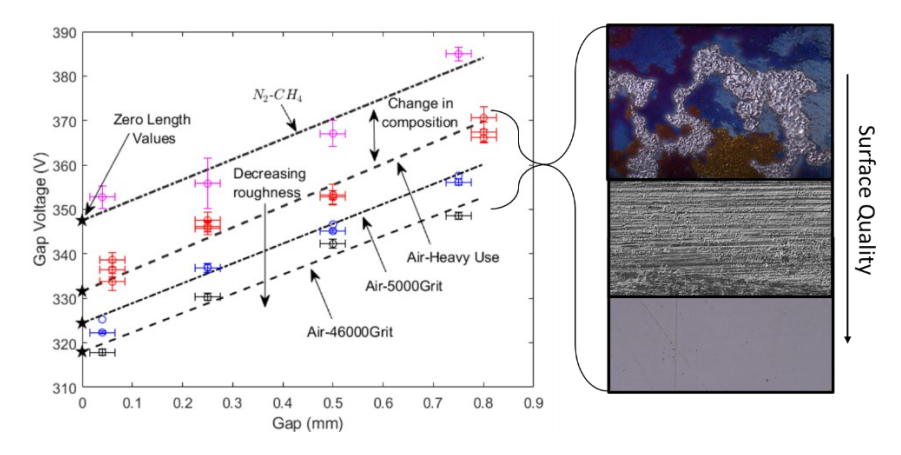


Fig. 3 Effect of composition and surface quality on the glow discharge sheath drop.

Smooth surfaces were found to decrease the sheath voltages while rough highly used electrodes had a significant increase, Images of the electrode surface under these different conditions were taken and shown in conjunction with the effect on extrapolation data.

The change to a methane mixture saw a further increase in the voltage drop, all of these changes are significant to the model results where the discharge energy, \dot{E}_{net} , is the most significant model parameter.

The effect of pressure change on glow discharge is shown in Fig. 4 and decreases regularly. Data reliable enough to be measured was captured up to 3 atm and a fit is shown up to 5 atm since some glow discharge is still possible for this range.

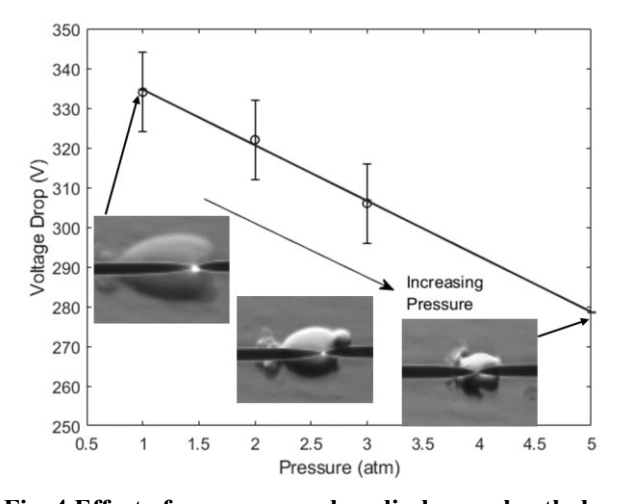


Fig. 4 Effect of pressure on glow discharge sheath drop

Arc discharge was also measured in a similar fashion however a single value of $15V \pm 2.5V$ measured over a pressure up to 20 atm. This value was not sufficient for the modeling result and was found to be only valid when the plasma is directly between the electrode tips. A higher value (30-60V) is necessary when arc plasma extends beyond the gap.

C. Model Application

Four spark conditions in Fig. 5 are used to show a significant range of possible spark - model solutions. Two conditions show pure glow discharge at 1 and 3 atm. The model predicts the overall size and finds relatively good agreement with the measured sheath losses. This represents an ideal case in which the spark is well behaved providing easy to measure kernels. However a discrepancy is seen when comparing the shape of the predicted propagation to the measurement. The model is seen to underpredict at early times and over predict at the later radius. This is attributed the constant sheath drop assumption made for this work. The plasma sheath may vary with time and will be one focus of future research.

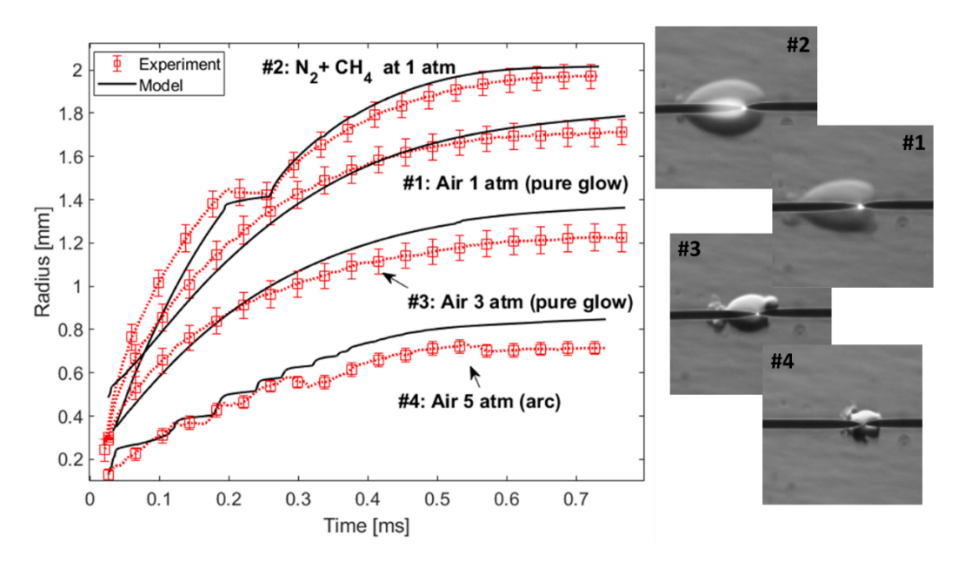


Fig. 5. Model results with images of kernel near end of discharge

Conditions with arc are more likely with increasing pressure and should be examined. At 5 atm there is significant arc discharge and required the use higher losses than the measured 15V. This is potentially a result of many effects but mostly because the spark escapes the gap causing either; the measured kernel to be underpredicted from hidden kernel growth (not in the imaging plane), and/or model over prediction from additional losses present as more electrode surface comes into contact with the plasma.

The second condition with the alternative composition operates primarily under glow discharge with a small amount of arc discharge (large discontinuity in data). In this case arc discharge only exist exactly in the gap (not shown) resulting very low thermal energy and no kernel growth at this point. The energy lost through the sheath mechanism must be close to the measured arc value for this case and suggest the efficiency of the arc phase depends on the length of the arc observed. The arc condition has a similar loss to the measured sheath measurement and the same effect of the glow discharge is present in this result where the model follows a slightly different trend.

In conclusion, the non-thermal losses for arc and glow plasma for several experimental conditions are observed and applied to a thermodynamic model. For Glow discharge, Model is observed to replicate the overall experimental propagation rate with the exception of some suspected time varying sheath effects. The arc discharge for some conditions can be accurately represented if higher than expected losses are used. Further study on the arc discharge should be done to better characterize such discharge and the interaction of this plasma with the electrode. It is suspected that the model is accurate in terms of characterizing the size the plasma kernel if accurate thermal energy are utilized. Future study should focus on improving the quality of input energies to this model.

Acknowledgments

Support from the National Science Foundation under Federal Award No. CBET-2039486 issued through Combustion and Fire System program (John Daily, Program Manager) is greatly appreciated

References

The following pages are intended to provide examples of the different reference types. All references should be in 9-point font,

- [1] Zembi, J., Cruccolini, V., Mariani, F., Scarcelli, R., and Battistoni, M., 2021, "Modeling of Thermal and Kinetic Processes in Non-Equilibrium Plasma Ignition Applied to a Lean Combustion Engine," Appl. Therm. Eng., 197, p. 117377. DOI 10.1016/J.APPLTHERMALENG.2021.117377.
- [2] Bogaerts, A., and Centi, G., 2020, "Plasma Technology for CO2 Conversion: A Personal Perspective on Prospects and Gaps," Front. Energy Res., 8, p. 111.
- [3] Ju, Y., and Sun, W., 2015, "Plasma Assisted Combustion: Dynamics and Chemistry," Prog. Energy Combust. Sci., **48**, pp. 21–83.
- [4] Haertel, B., von Woedtke, T., Weltmann, K. D., and Lindequist, U., 2014, "Non-Thermal Atmospheric-Pressure Plasma Possible Application in Wound Healing," Biomol. Ther. (Seoul)., 22(6), p. 477. DOI 10.4062/BIOMOLTHER.2014.105.
- [5] Economou, D. J., 2014, "Pulsed Plasma Etching for Semiconductor Manufacturing," J. Phys. D. Appl. Phys., 47(30), p. 303001.
- [6] Sher, E., Ben-Ya'Ish, J., and Kravchik, T., 1992, "On the Birth of Spark Channels," Combust. Flame, **89**(2), pp. 186–194. DOI 10.1016/0010-2180(92)90027-M.
- [7] Michler, T., Toedter, O., and Koch, T., 2020, "Measurement of Temporal and Spatial Resolved Rotational Temperature in Ignition Sparks at Atmospheric Pressure," Automot. Engine Technol., **5**(1–2), pp. 57–70. DOI 10.1007/s41104-020-00059-w.
- [8] Kawahara, N., Hashimoto, S., and Tomita, E., 2017, "Spark Discharge Ignition Process in a Spark-Ignition Engine Using a Time Series of Spectra Measurements," Proc. Combust. Inst., **36**(3), pp. 3451–3458. DOI 10.1016/j.proci.2016.08.029.
- [9] Aragón, C., and Aguilera, J. A., 2008, "Characterization of Laser Induced Plasmas by Optical Emission Spectroscopy: A Review of Experiments and Methods," Spectrochim. Acta Part B At. Spectrosc., **63**(9), pp. 893–916. DOI 10.1016/J.SAB.2008.05.010.
- [10] Arkhipenko, V. I., Kirillov, A. A., Safronau, Y. A., Simonchik, L. V., and Zgirouski, S. M., 2012, "Plasma Non-Equilibrium of the DC Normal Glow Discharges in Atmospheric Pressure Atomic and Molecular Gases," Eur. Phys. J. D, 66(10), p. 252. DOI 10.1140/epid/e2012-30359-x.
- [11] Askari, O., 2018, "Thermodynamic Properties of Pure and Mixed Thermal Plasmas Over a Wide Range of Temperature and Pressure," J. Energy Resour. Technol. Trans. ASME, **140**(3). DOI 10.1115/1.4037688.
- [12] Askari, O., Beretta, G. P., Eisazadeh-Far, K., and Metghalchi, H., 2016, "On the Thermodynamic Properties of Thermal Plasma in the Flame Kernel of Hydrocarbon/Air Premixed Gases," Eur. Phys. J. D, **70**(8), p. 159. DOI 10.1140/epjd/e2016-70195-4.
- [13] Swett, C. C., 1951, NACA Research Memorandum Spark Ignition of Flowing Gases II-Effect of Electrode Parameters on Energy Required to Ignite A Propane-Air Mixture.